Australian Government
Department of Defence
Defence Science and
Technology Organisation

Detection of Accelerating Targets in Clutter Using a De-Chirping Technique

H.T. Tran, R. Melino, and S. Kodituwakku

National Security and Intelligence, Surveillance and Reconnaissance Division

Defence Science and Technology Organisation

DSTO–RR–0399

ABSTRACT

Accelerating targets induce chirped signals in the radar backscatter signal which cannot be efficiently detected by the direct application of the traditional Fourier transform. In this report, we propose a method based on a de-chirping factor and the Fourier transform for detecting accelerating targets in land or sea clutter environments. The method is found to be simple, yet highly effective. The results are demonstrated with both simulated and real data.

APPROVED FOR PUBLIC RELEASE

Published by

DSTO Defence Science and Technology Organisation
PO Box 1500
Edinburgh, South Australia 5111, Australia

Telephone: 1300 333 362
Facsimile: (08) 7389 6567

© *Commonwealth of Australia 2014*
AR No. AR-015-961
June, 2014

APPROVED FOR PUBLIC RELEASE

Detection of Accelerating Targets in Clutter Using a De-Chirping Technique

Executive Summary

Accelerating targets introduce chirped signals in the radar backscatter signal that cannot be efficiently detected by a direct application of the traditional Fourier transform (FT). However, by applying a simple de-chirping factor, followed by a Fourier transform, they can be detected as efficiently as the case of the Fourier transform detecting pure-tone signals. Furthermore, the spectrum of most clutter signals tend to defocus upon the application of both of these processing techniques providing an extra gain in the achievable signal-to-clutter ratio (SCR) for accelerating target detection.

The proposed de-chirping technique is simple in terms of implementation, and was found to perform better than alternative techniques such as those based on the integrated cubic phase functions, at least in the case of single target detection with the linear frequency modulated (LFM) waveform. This is because the technique is linear and thus does not generate added false alarms or noise-like components in the processing. Compared with its most closely related technique - the novel Fractional Fourier Transform (FrFT) technique - their performances are very similar, except that the de-chirping technique algorithm is easier to implement making the processing faster.

The work also includes detailed detection algorithms for single targets, and for multiple targets in the same range bin, with estimates of computational costs expected to be well within the computational capacity of most modern fielded radars. Results achieved based on simulated as well as real data are indeed very promising.

THIS PAGE IS INTENTIONALLY BLANK

Authors

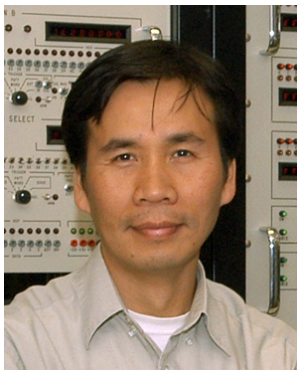

Dr. Hai-Tan Tran
National Security and ISR Division

Hai-Tan Tran graduated from the University of Sydney in 1990 and obtained his PhD degree from the Australian National University in Canberra in 1993, in the field of nonlinear guided-wave optics. He spent the next three years as a postdoctoral research fellow in the Mathematics Department of the Australian Defence Force Academy, also in Canberra, working on the theory and simulation of spatial optical solitons and light-induced optical switching in nonlinear dielectric media, before joining the National Security and ISR Division of DSTO, Edinburgh, in 1996. His current research interests include high-resolution radar imaging, automatic target recognition, radar electronic protection, and various topics in signal processing.

Mr. Rocco Melino
National Security and ISR Division

Rocco Melino received a Bachelor Degree in Electronic Engineering from the University of South Australia in 1999 and has a Masters Degree in Signal and Information Processing from the University of Adelaide. He has been working for the National Security and ISR Division of DSTO since 1999, in the branch of microwave radar. His research interests include radar automatic target recognition, radar modelling and signal processing.

Dr. Sandun Kodituwakku
National Security and ISR Division

Sandun Kodituwakku received a Bachelor of Engineering (Electrical and Electronic) from the University of Adelaide in 2006, and a PhD in the field of signal processing from the Australian National University in 2012. He works as a radar signal processing researcher at DSTO since 2011.

THIS PAGE IS INTENTIONALLY BLANK

Contents

Figures

Tables

1 Introduction

This work addresses the question of how airborne accelerating targets in the presence of land and sea clutter can be most efficiently detected by a pulsed Doppler radar when low computational cost is vitally important.

Target acceleration matters for two important reasons: (1) it may impact on the probability of target detection, and thus on tracking, for radars in which the signal processing assumes constant target range rate (or radial velocity) employing Fourier transform processing for coherent integration; (2) target acceleration is a common and significant target attribute present in many scenarios of interest. Most traditional radars attempt to minimise the degrading effects of target acceleration by restricting the coherent integration interval (CPI)[1] to relatively small values, thus limiting the coherent integration gain and hence the detection performance achievable.

The use of the traditional Fourier transform (FT) for target detection in coherent radars is well known. So is the fact that it works most efficiently only on constant or nearly constant (radial) velocity targets that impart pure-tone modulated signals in the radar backscatter. For accelerating targets inducing chirped signals, whose instantaneous frequency varies approximately linearly over a typical CPI, a frequency line in the FT-based spectrum would become spread out, the extent of which directly depends on the bandwidth of the induced chirp signals and the duration of the dwells. The spreading reduces the processing gain, and hence a degraded detectability of the target. Figure 1 describes the gain reduction in the FT for a typical radar PRF and various acceleration levels.

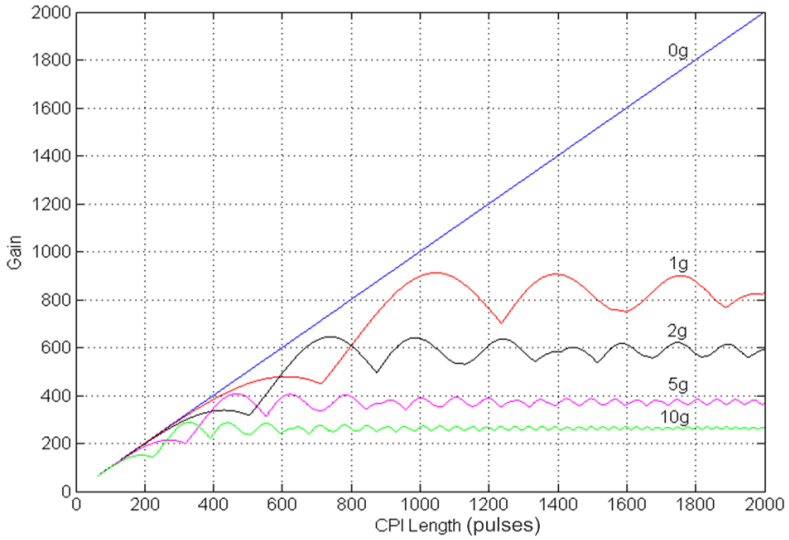

Figure 1: *Coherent gain of the traditional Fourier transform versus CPI length, for various target accelerations for a* 3 *GHz radar with a* 10 *kHz PRF.*

In most scenarios of interest, target acceleration may result from several types of target-radar relative motion that may be loosely summarised as: (1) *Linear acceleration* by the

[1] A CPI is a time interval over which the signal is coherently integrated to maximise the signal gain in the receiver.

target along the velocity vector, or equivalently by radar platform. The change of speed would result in a projected acceleration that, apart from degrading the coherent integration gain, could also result in a track bifurcation if the tracker uses range rate in its track initiation logic. (2) *Lateral acceleration* perpendicular to the velocity vector - the target is turning and hence inducing an acceleration in the radar line of sight. The number of potential looks on the target during the turning depends on the exact kinematics of target, and may be significantly impacted if the acceleration effect is not sufficiently compensated. (3) *Weave manoeuvres* - the target mean velocity is constant but it undergoes a sequence of reversing the sign of its lateral acceleration, with the intention of degrading the radar track quality or effecting a 'break lock'. (4) *Dog-fights* - in which two or more objects undergoing an extended sequence of related (but not identical) accelerations; the radar may be associated with one of the objects. All these types of motion result in chirped signals in the radar receiver that must be appropriately processed.

Chirp detection has been an active area of research for many years. There are statistically optimal techniques for chirp detection such as the maximum likelihood estimator (MLE) proposed by Abatzoglou in [1]; this however is computationally demanding in the two-dimensional (2D) maximisation involved, and may not be suitable for most real-time applications. The drawback was resolved to some extent by reducing the problem to two 1D solutions using the discrete polynomial transform (DPT) described in [2], which can produce good results for single-component chirped signals in low noise conditions.

There are also bilinear time-frequency techniques for chirp detection, such as those based on the well-known Wigner-Ville distribution proposed by Wood [3] and Barbarossa [4], or the Radon-ambiguity transform (RAT), explored in [5]. Furthermore, new techniques based on cubic phase functions, such as those discussed in [6, 7, 8, 9], are computationally efficient and perform well in noisy conditions. This type of techniques perform optimally in some sense, because they are essentially built around the idea of matched filtering to a single linear chirp signal. However, when multiple chirp components are present in a received signal, cross terms are always a problem, giving rise to spurious targets and hence *artificially introduced* false alarms for target detection algorithms. This is undoubtedly an undesirable effect for radar detection. Extra and sophisticated processing can be used, an excellent example of which has been reported recently by Wang *et al.* in [9], to reduce (not to totally eliminate) spurious targets. These measures, however, always come with an unavoidable extra computational cost. More importantly, detection performance using bilinear techniques may depend on how 'dense' the signal components are in their parameter space and the actual detector employed.

The authors believe that linear techniques still offer the best chance of detecting multiple-component chirped signals, free of spurious targets. In that pursuit, we have attempted to apply the Fractional Fourier transform (FrFT) to the problem of detecting an accelerating target in clutter, as reported in [10]. The FrFT, which can be viewed as a generalisation of the traditional FT, has been proposed earlier for use in the detection of audio chirped signals [11] and accelerating targets by pulsed Doppler radars in the presence of clutter [12]. In terms of coherent processing gain, the FrFT can be optimum for linear chirped signals, in the same manner that the traditional FT is optimum for pure-tone signals. Furthermore, when the FrFT is applied to clutter, the wide-sense stationary property of clutter means that the clutter spectrum is defocussed, the extent of which depends on the transform order used in the FrFT which in turn depends on the acceleration

of the target being detected.

In this report, we simplify the FrFT-based idea by replacing it with a linear de-chirping technique, and demonstrate with Monte-Carlo simulations that, with respect to our previous work based on the FrFT [10], detection performance is unchanged, with a computational cost at least 50 times lower. We present detection algorithms for both single and multiple targets in clutter background, based on a metric called 'the kurtosis' or direct 2D search, and a version of the CLEAN technique. As a basic comparison with known techniques, especially those based on cubic phase functions, we demonstrate with a simulated example in which the signal contains a single LFM signal that detection performance of the proposed technique in a noise-limited scenario is better than that reported in [9]. Another advantage of our proposed technique is its relative insensitivity to the 'density' of chirp components present, and that it does not impose extra conditions or requirements on the choice of CFAR detector employed.

2 Radar Environment and Signal Models

Our current problem assumes an airborne pulsed Doppler radar, in a look-down scenario, with its receiver employing possibly a number of range bins and a CPI of N time samples, which is supposed to be both large enough to capture the acceleration of a target and short enough to be compatible with the baseline processing of the radar correcting for 'range walk' across adjacent range bins.[2] Furthermore:

- detection processing is required at each CPI, and thus the choice of processing across the CPIs may be an additional option but not a replacement of the CPI-level processing
- each range bin is Doppler processed separately, using the same algorithms proposed herein
- for simplicity, only schematic radar antenna gain patterns are currently included in this study.

Within this context, ground or sea clutter can be expected to have a rather limited Doppler extent depending on the range bin being processed, antenna gain pattern and look angle, platform speed, and altitude. Signal data structures such as spectrograms are not involved, and only Doppler processing for a CPI needs be considered. For the sake of simplicity, we start with the case of no more than one accelerating target present in any one range bin and any one CPI. The extension to multiple targets is discussed separately in the next section.

In continuous form, the total signal in the radar receiver typically consists of three components

$$u(t) = s(t) + c(t) + \nu(t),$$

[2]Research on coherent target detection across multiple range bins and over long CPIs is currently one of our topics for active research, and will be reported elsewhere.

of the target signal itself, the clutter, and the receiver thermal noise, respectively. The thermal noise component $\nu(t)$ is assumed to be simply Gaussian white noise with its amplitude set to 10 dB below the clutter. The following subsections describe the models being used for $s(t)$ and $c(t)$ in some detail.

2.1 Target Model

Assuming that the target has a constant linear acceleration a during the CPI, the target velocity is $v = v_0 + at$, where v_0 is initial velocity. In the monostatic radar configuration, the sampled radar return signal from the target after pulse compression can readily be shown to take the form

$$s(t_n) = A_n \exp\{2\pi i t_n (f_d + a t_n/\lambda)\}, \quad n = 1, 2, \ldots, N \tag{1}$$

where A_n are the return signal magnitudes governed by the radar range equation (and perhaps the sinc-shape response of the matched-filter pulse compression processing), λ is the radar wavelength, and $f_d = 2v_0/\lambda$ is the baseline target Doppler frequency corresponding to initial target velocity v_0. Here, n is an integer representing the sampling time index, N is the number of time samples in the CPI, or 'CPI length' as mentioned earlier. For simplicity, we also assume that signal reception is free of blind zones in the region occupied by the target. The sampling rate for each range bin , i.e. the inverse of the sampling period, also known as the pulse repetition frequency or 'PRF', determines the maximum unambiguous velocity of the system.

In this work, the target signal amplitudes A_n is modelled as Swerling I type. As a reminder, a Swerling I type target has a constant A_n for all values of n in a CPI, and for all CPIs of a time-on-target, but fluctuates according to a Chi-square distribution from scan to scan. The interested reader is referred to [13] for more detail. For the applications described herein, detection processing is required for each CPI, and the effects of scan-to-scan target fluctuation are not considered.

Examples of possible accelerating target spectra, with time-domain signals described by (1), are shown in Figure 2. These Doppler spectra are based on the traditional Fourier transform, which feature smeared out 'plateaus', rather than well focused peaks as in the case of pure tone signals. The width of such a plateau is a measure of the bandwidth of the acceleration induced Doppler chirp.

Recently, Yasotharan *et al.* [14] reported a quantitative assessment of the degradation of the FT when applied to accelerating targets which typically produce a linear chirp during a CPI. An extension of the results contained in [14] are shown in Figures 1 and 3. The gain selected for plotting in these figures corresponds to the maximum point on the plateau. While the oscillatory behavior of the gain factor in Figure 1 is the direct result of this choice for the gain factor, the mean gain factor quickly saturates, as the CPI length is increased, to a value that monotonically decreases with target acceleration. Figure 3 shows a similar plot but for a fixed acceleration and varying PRF. The inverse relationship between CPI and PRF means that the effects of acceleration are greater for low PRF's with gain saturation effects similar to those seen in Figure 1.

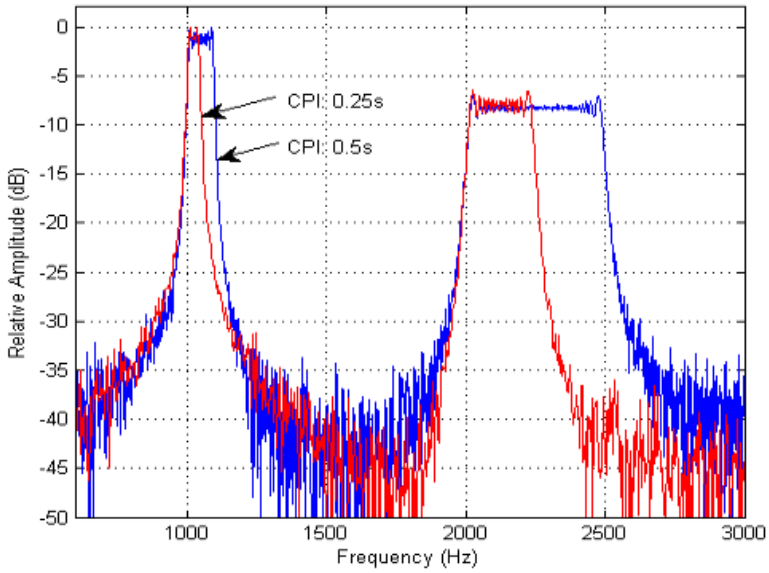

Figure 2: *Fourier spectra of two chirp signals from scatterers with accelerations of* $2g$ *and* $10g$*, and the effect on chirp bandwidth for different CPI's.*

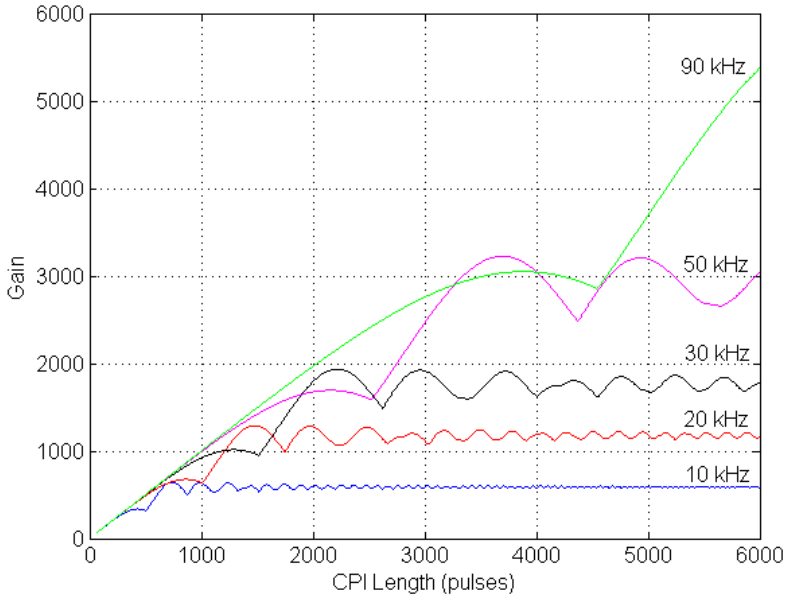

Figure 3: *Coherent gain of the traditional FT versus CPI length, for varying PRFs (from 10 kHz to 90 kHz), a fixed target acceleration at* $2g$*, and for a* 3 *GHz radar.*

2.2 Clutter Model

In this work, we simply use a standard surface clutter model which can provide a necessary component of the composite radar backscatter signal, to which the de-chirping technique or the novel tool of the FrFT can be applied. The model is often referred to as the NECAPS model [15], which has also been summarised in [10].

Table 1: *System and scenario parameters for clutter simulation*

Carrier Frequency, f_c	3 GHz
Pulse Repetition Freq, PRF,	40 kHz
Polarisation	horizontal
Platform Velocity, v_p	100 m/s
Antenna Look Direction	forward
Sea State, ss	3, 5
Wave Direction, γ	0°
Antenna Beamwidth, $\Delta\theta$	6°
Range Bin Size, Δr	150 m

An Example of simulated sea clutter using the NECAPS model, with typical scenario parameters as in Table 1, is shown in Figure 4. The clutter spectra are for sea states 3 and 5, for which a CPI of 0.5 s has been used. Note that:

1. Both mainlobe and sidelobe clutter are considered in these examples, employing a simple sinc antenna pattern, with sidelobe levels -13 dB below mainlobe. With a forward looking antenna, mainlobe clutter occurs at the upper edge of the clutter region, causing an asymmetric look to the clutter spectrum.

2. By the nature of our problem, only one range bin containing both mainlobe and sidelobe clutter is investigated with no clutter beyond the clutter patch. For simplicity, only those clutter patches inside $\pm 30°$ of the look angle are included.

3. Also for simplicity, and to investigate how clutter behaves under the de-chirping technique and the FrFT, no noise is added to the simulated signal and no FFT windowing has been applied.

3 Signal Processing Techniques

In this section, we briefly describe the de-chirping techniques, discuss their properties and effects when applied to target and clutter signals, and discuss their similarities and differences with the more sophisticated Fractional Fourier Transform (FrFT). Since the detection problem involves estimating the target acceleration as well as the average (or initial) target velocity, it is in general a two dimensional detection problem, which may

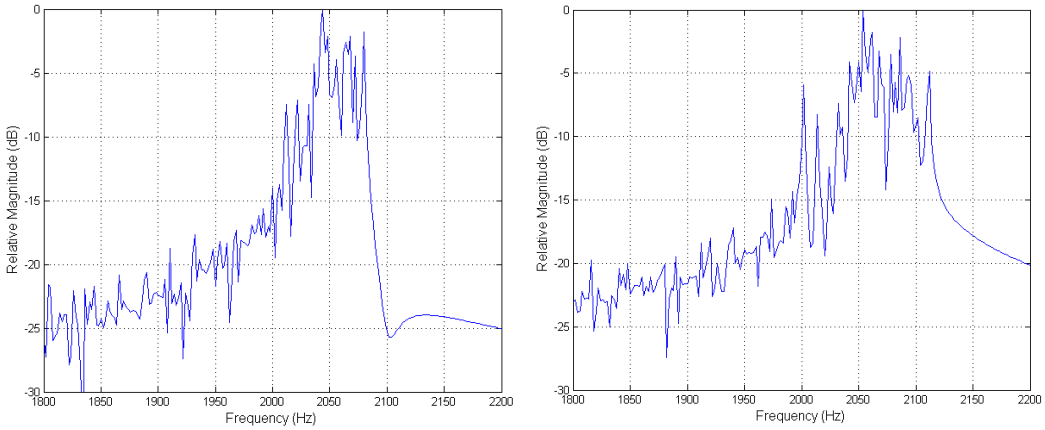

(a) For sea state 3 (b) For sea state 5

Figure 4: *Examples of Doppler spectra of simulated clutter, sea states* 3 *and* 5*, showing both mainlobe and sidelobe clutter.*

be solved directly by a 2D search, or by reducing it to an alternative algorithm involving two 1-D searches, as will be described in detail later in this section.[3]

3.1 Review of Known Techniques

For convenience of comparison with most relevant techniques, we review three classes of techniques: those based on the auto-correlation function, on cubic phase functions (CPF), and the fractional Fourier transform (FrFT).

3.1.1 Auto-correlation and Cubic Phase Functions

By definition the Wigner-Ville distribution, W, of a signal $x(n)$ can be written generally as

$$W(n,\omega) = \sum_m x(n+m/2)x^*(n-m/2)e^{-j\omega m} \tag{2}$$

where ω represents the instantaneous frequency. The projection of W at an arbitrary angle (i.e. line integration) gives the Radon Transform of W, which is known as the Radon-Wigner transform (RWT), as discussed by Wood [3] and Lohmann [16].

Similarly, the Ambiguity Function, AF, for the signal $x(n)$ can be also be generalised as

$$AF(n,\omega) = \sum_m x(m+n/2)x^*(m-n/2)e^{-j\omega m} \tag{3}$$

Again, the projection of AF at arbitrary angles gives the Radon Transform of AF and the so-called Radon-Ambiguity Transform (RAT), as described by [5]. The RAT and RWT

[3] Application of the FrFT itself in this problem has been discussed elsewhere, such as in [10], and will not be described in any great detail here.

produce lines in the time-frequency space, which are captured by the Radon transform. The difference between the RAT and RWT is that all lines in the RAT pass through the origin of the AF.

While these are excellent filters for isolated (in their parameter spaces) linear chirp signals, a major disadvantage with them is that they are second-order bilinear transforms that can produce strong cross terms when multiple chirped components exist in the signal, especially when the chirps heavily overlap. Furthermore, the computational cost carries an added loading as the Radon transform requires Cartesian-to-polar coordinate transformations and interpolations.

The paper by Wang *et al* [9] extends the ideas of the RWT and RAT by defining a 'cubic phase function' (CPF) as,

$$CPF(n,\Omega) = \sum_m x(n+m)x(n-m)e^{-j\Omega m^2} \tag{4}$$

with Ω representing the (instantaneous) frequency rate, and m being a running positive integer index such that $(n-m)$ and $(n+m)$ covers all available samples of the signal $x(n)$.

As a note on the 'historical background' and relevance of the CPF in our current problem, it could be remarked that the term 'cubic phase' may be confusing as the technique was originally applied to the detection of instantaneous frequency rate for cubic phase signals [7], i.e. signals with a chirp rate (or acceleration) varying linear with time. In our Report, chirp rate is assumed constant, hence the signal phase is a quadratic function with time. The application of the CPF to quadratic phase signals produce lines parallel to the time axis in the time-frequency plane, which are useful for their detection, as discussed in [9]. This is the main difference to the RAT and RWT which produce straight lines at arbitrary angles.

However, as a bilinear filter, 'auto-terms' produce lines parallel to the time axis, while cross-terms may produce peaks that are time varying. To overcome this problem and to exploit the property that the auto-terms are straight lines parallel to the time-axis, the so-called integrated cubic phase function (ICPF) is used, which is described by Wang *et al* as

$$ICPF(\Omega) = \sum_n |CPF(n,\Omega)|^2. \tag{5}$$

This summation integrates the energy of the auto-terms over time forming a peak in the Ω space while suppressing the peaks formed by the cross-terms. From here a simple detection scheme can be used to determine Ω.

The ICPF is indeed an interesting filter. However, further detailed investigation is still necessary for a more quantitative characterisation of the behaviour of the CPF when applied to multiple-component chirped signals. It can be anticipated that the CPF may also run into the difficulty of cross-terms with such signals. Numerous false targets can still be created which are strong enough to compete with the auto-terms of the actual chirp components and hence may significantly degrade detection performance.

3.1.2 The Fractional Fourier Transform

The fractional Fourier transform (FrFT), first proposed by Namias [17], is a relatively new tool for signal processing. It can be described as a generalisation of the classic Fourier transform in which a linear chirp signal in the real time domain becomes a pure tone signal again in the suitably rotated time-frequency domain. An attractive advantage of the FrFT is that it is a linear transform, and hence is free from the problem of cross coupling between multiple frequency components of the signal.

For a time signal $s(t)$, the continuous form of the FrFT is defined as

$$S_\alpha(u) = \mathcal{F}_\alpha\{s(t)\} = \int_{-\infty}^{\infty} K(\alpha, u, t)\, s(t)\, dt, \tag{6}$$

where the kernel function is

$$K(\alpha, u, t) = \begin{cases} \left(\frac{1-i\cot\alpha}{2\pi}\right)^{1/2} \exp\{i\frac{\cot\alpha}{2}(u^2+t^2)\} \exp\{-i\frac{u}{\sin\alpha}t\}, & \alpha \neq n\pi, \\ \delta(t-u), & \alpha = 2n\pi, \\ \delta(t+u), & \alpha = (2n-1)\pi, \end{cases} \tag{7}$$

and where α is called the *order* of the transform, or 'transform order', which can also be interpreted as an angle of rotation in the time-frequency plane. For $\alpha = 0$ (i.e for $n = 0$ in Equation 7), we have $S_0(u) = s(u)$ which is the time-domain signal itself. For $\alpha = \pi/2$, we have $\cot\alpha = 0$ and $\sin\alpha = 1$, and $S_{\pi/2}(u)$ reduces to the traditional Fourier transform $S(u) = S(\omega)$ of $s(t)$. (Here, $\omega = 2\pi f$ denotes angular frequency.) The traditional FT is a rotation of the time signal through an angle of $\pi/2$ in the time-frequency plane. A rotation through some other angle gives a generalised or 'fractional frequency' spectrum of the signal at that angle, with (angular) fractional frequency denoted by u.

Properties of the FrFT and its numerical implementation have been summarised in [18] and the numerous references therein. For convenience of discussion in the current Report, we here include the most relevant properties and effects of the FrFT.

For the correct transform order α, the FrFT can achieve the maximum integration gain of N, which is the gain achievable by the traditional FT on a pure tone signal of N samples. Note also that a shift of the time reference of the signal $s(t)$ would correspond to a (linear) translation in the fractional frequency u domain, and due consideration needs be given to this property of the FrFT in applications.

In applying the FrFT to the detection of an accelerating target, note that such a target with constant (radial) acceleration a produces a constant chirp rate of $c_r = a/\lambda$, and the instantaneous target Doppler frequency is $f = f_0 + c_r\, t$ where f_0 is an initial Doppler frequency.

To spectrally compress such a chirp, the optimal transform order α that should be used is related to c_r through

$$\alpha = \frac{\pi}{2} + \beta = \frac{\pi}{2} + \tan^{-1}(D\, c_r), \tag{8}$$

in which the scale factor D due to the discretisation of the time-frequency plane is related to the time and frequency resolutions δt and δf by [11]

$$D = \left(\frac{\delta f}{\delta t}\right)^{-1} = \left(\frac{N}{PRF^2}\right). \tag{9}$$

With an optimal rotation angle β as expressed in (8), the signal would appear like a 'pure tone' along the 'fractional time' domain, or equivalently as an optimally compressed spike in the 'fractional frequency' domain.

In terms of the output frequencies, the de-chirping technique with the correct de-chirp rate can produce a focused peak at a physically meaningful frequency, which is also equal to the instantaneous frequency at the time origin of the chirp; whereas the FrFT would produce a 'fractional frequency', for a transform order α corresponding to the correct target acceleration. Nevertheless, in typical applications, the numerical differences between the output frequencies of the two techniques are negligible.

3.2 Proposed De-Chirping Technique

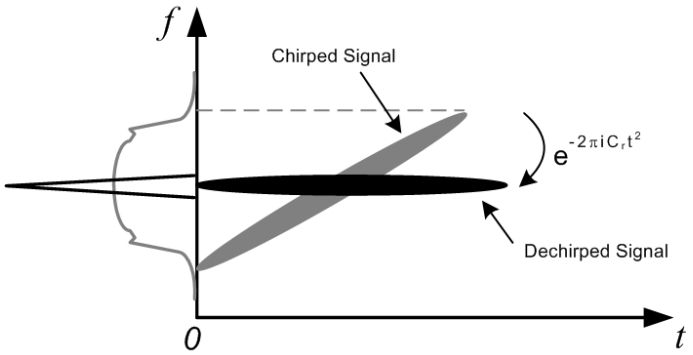

Figure 5: *Illustration of the rotation of a chirped signal by de-chirping.*

To detect a chirped signal in noise or clutter, the non-linear phase of the signal can be corrected by multiplying it with a de-chirping factor followed by an application of the FFT. Assuming the target's acceleration a is approximately constant during the CPI, the de-chirping factor can take the linear form

$$\exp(-2\pi i c_r t_n^2), \quad n = 1, 2, \ldots, N,$$

where c_r $(= a/\lambda)$ is the 'de-chirp rate'. If c_r is equal to the true chirp rate of the target signal, the de-chirping factor effectively reduces the linear chirped target signal to a pure tone signal at a frequency equal to the instantaneous frequency at the time origin of the chirp. It is most convenient to setup the time vector $\{t_n\}$, $n = 1, 2, \ldots, N$ such that the time origin is at the center of this vector. Schematically, the de-chirp factor rotates the signal in the time-frequency plane as depicted in Figure 5.

Figure 6 demonstrates the effectiveness of the technique on real data collected by an experimental radar from an accelerating helicopter (Bell 206L3) target, for approximately 0.65 s, with a PRF of 33.33 kHz. In Figure 6(a), a spectrogram of the data indicates an acceleration of about 2.21 m/s^2. With that approximate prior knowledge, the de-chirping technique produces a well compressed spectrum shown by the red line in Figure 6(b), while the traditional FT produces a much more smeared out spectrum shown in blue. In terms of improvement in SNR, the de-chirping technique clearly produces a very significant gain; the exact measure of which depends on how SNR is defined for this particular problem.

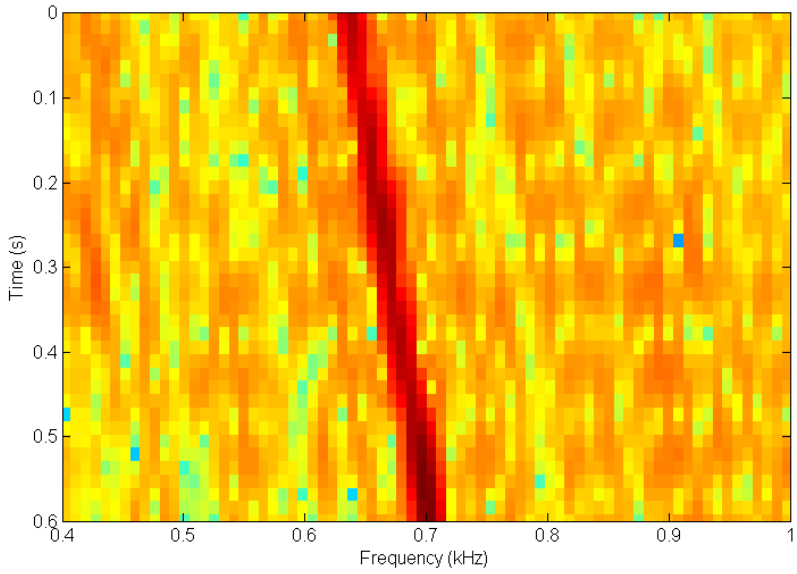

(a) Spectrogram (with STFT)

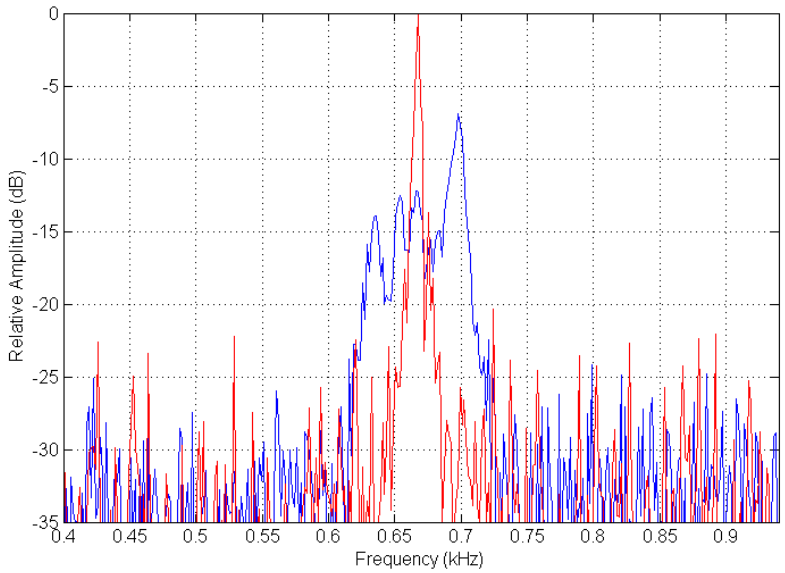

(b) Spectra by traditional FT (blue), and de-chirping technique (red)

Figure 6: *De-chirping technique on received signal from a real helicopter target.*

Figure 7 shows a typical comparison of the effect on clutter for the FrFT and the de-chirp techniques: the effects are essentially the same. This similarity can be explained by noting that the FrFT is essentially a de-chirping technique with additional scaling and chirping factors in the fractional frequency domain.

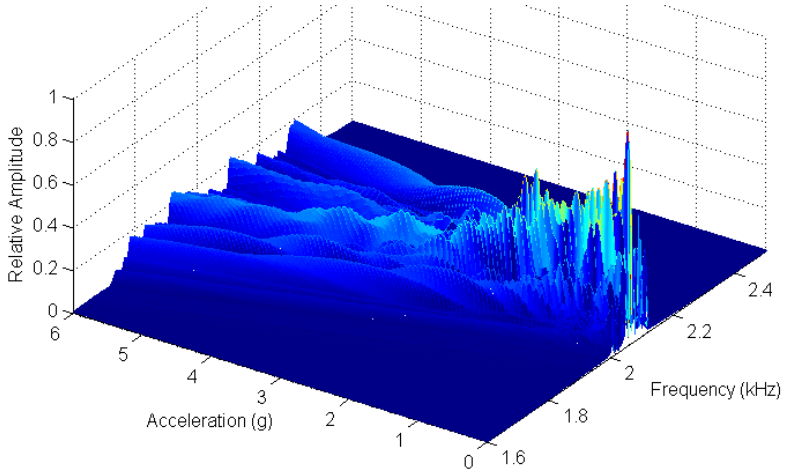

(a) FrFT on clutter

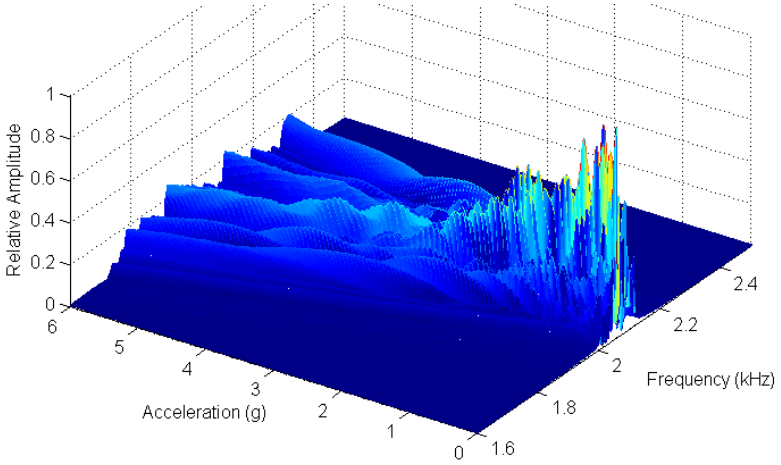

(b) De-chirping technique on clutter

Figure 7: *Effects on clutter of the FrFT and de-chirping techniques, for simulated sea clutter, sea state 5.*

The question of how to determine the best de-chirp factor is common for both the FrFT and this technique, and will be discussed in the following subsection on detection algorithm.

Lastly, if target acceleration can not be approximated as constant during a CPI, then the proposed acceleration processing will result in a loss of peak SNR and thus reduced

detectability. If the loss is significant, then it will be necessary to include a more complex motion model into the signal processing.[4]

3.2.1 Single-Target Detection

First, consider the case where one target is to be detected in any CPI. The solution to the problem includes estimates of two target parameters. The first one is the transform order α in the FrFT technique, or equivalently the de-chirp rate c_r of the de-chirping technique, which are directly related to target acceleration. The second parameter to be determined is target Doppler frequency f_d (or equivalently, its radial velocity) in that CPI. Thus, generally a direct 2D search over a certain region of the Doppler frequency-acceleration plane would have to be done. It is also possible to perform the 2D search by reducing it to two 1D searches. The first 1D search involves a peak detection to estimate c_r. The second 1D search is then carried out over the FT output of the signal at that acceleration to estimate f_d.

For convenience, we here use the de-chirping technique, instead of the more computationally intensive FrFT. Suppose c_{r0} denote the correct de-chirped rate to be solved for. As the de-chirp rate c_r varies through c_{r0}, the FT spectrum of the de-chirped signal changes from unfocused to most focused and back to unfocused characteristics, as illustrated in Figure 8. The detection and localisation of the peak in that frequency versus chirp rate plane would be the objectives of the currently sought algorithm.

Now, consider the estimation of c_{r0}. There are a number of test statistics that may be used to characterise the sharpness of a spectrum, including the fractional auto-correlation, the kurtosis, and the singular value decomposition of the auto-correlation, as discussed in [2, 19, 20, 21, 22]. We have found that the kurtosis, which is a fourth-order statistic of the spectrum, is the best choice for its low computational cost and reasonably high performance.

For a general non-negative real function $x(t)$ treated as a distribution, the kurtosis is a measure of shape and is defined as

$$\mathcal{K} = \frac{E\{(x(t) - \mu)^4\}}{\sigma^4} - 3,$$

where E denotes the expectation operation, μ is the mean, and σ^2 is the variance of $x(t)$. $\mathcal{K}$ takes larger values for 'spikier' distributions. For data containing only noise, $\mathcal{K} = 0$.

As an example, Figure 9 shows $\mathcal{K}$ for a chirped signal corresponding to an accelerating target of $5g$, at SNR of -6 dB (with no coherent integration gain), -9 dB and -12 dB. It can be seen that: (1) the kurtosis peaks at the true acceleration; and (2) although the value of $\mathcal{K}$ changes with SNR, its shape does not significantly change for SNRs greater than about -9 dB. Even at SNR of -12 dB, a global peak still features near the correct acceleration, despite the fact that noise effects begin to dominate. These properties indicate that the kurtosis is a viable and effective choice for the detection of target acceleration.

As a measure of reducing the error on the estimate for c_{r0} in numerical implementation, a parabolic curve fitting through three points near the peak of the kurtosis curve may be

[4]Non-linear chirp detection techniques are currently an active research topic at DSTO.

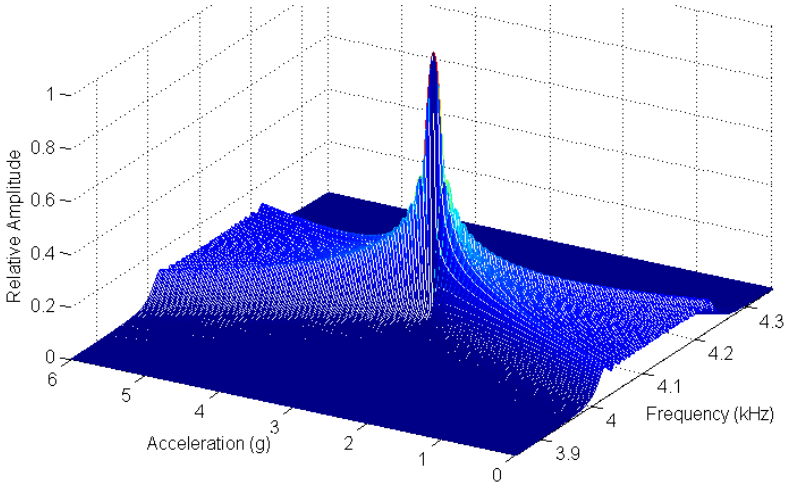

Figure 8: *Spectrum of the de-chirped signal for varying accelerations.*

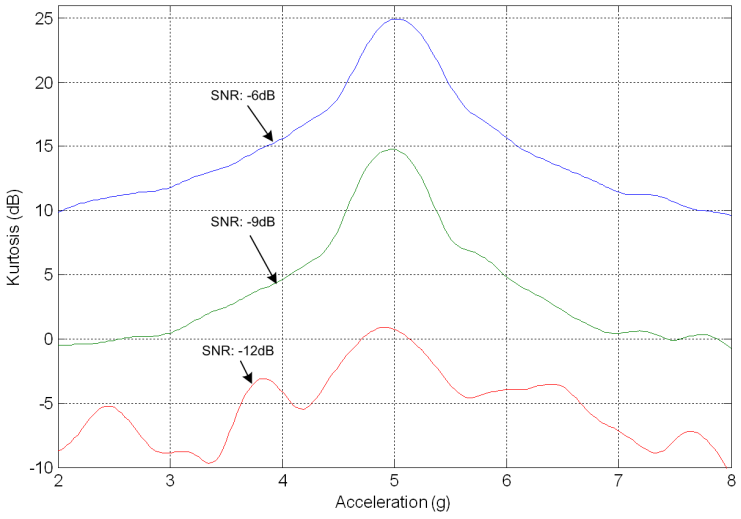

Figure 9: *Kurtosis for a chirp signal corresponding to a target with an acceleration of* 5*g for various SNR*

performed, and the c_r value corresponding to the peak of the parabola may be used as a refined estimate $\hat{c}_{r0}$.

After the estimation for target acceleration, $\hat{c}_r0$, a second 1D search for target Doppler frequency can be achieved with a traditional CFAR detection processing on the output of an FT application to the signal de-chirped with $\hat{c}_{r0}$.

The estimates for c_{r0} and f_d could also be obtained by one of many other optimisation algorithms, and any implementation of these techniques to an operational system should include a review of both the appropriate search algorithm and a determination of the acceptable losses which will determine the accuracy required for the search.

3.2.2 Multiple-Target Detection

When multiple accelerating targets are present in a CPI, Figure 8 would be replaced with a similar one with multiple peaks, each corresponding to a single target at which the de-chirping is best matched. The direct 2D search approach would be most appropriate to detect and locate them.

When the magnitudes of the target returns are also diverse and their parameters are similar enough (i.e. 'denser') in the Doppler-acceleration space, a stronger target may 'obscure' the weaker ones and prevent their detection. To provide for such cases, the CLEAN technique [23, 24, 25] could be used to detect and extract the targets sequentially, in the order of decreasing integrated signal magnitudes. The algorithm is as follows:

1. First, a 2D plot similar to Figure 8 is computed over a region of interest in the Doppler-acceleration space.

2. The largest peak over the 2D region is determined.

3. CFAR detection processing is performed along the frequency spectrum cut through the largest peak (at a constant value of acceleration).

4. The target is extracted by the CLEAN processing.

The process is repeated to detect the next weaker targets, until no more targets can be detected at a certain threshold according to CFAR detection theory. On the other hand, if targets are known a priori to be well separated, either in frequency or in range, then the CLEAN processing may not be necessary.

The detection scheme will be demonstrated with examples with simulated data in the next section. Note that the 'mesh size' of the 2D plot in step 1 would determine the accuracy of the Doppler-acceleration estimates of the target. To improve the accuracy of the acceleration estimate in particular, a finer local mesh may be used in the vicinity of the largest peak.

3.3 A Comparative Discussion

3.3.1 Performance of ICPF and De-Chirping Techniques

The dechirping technique proposed provides a useful tool for detecting single and multiple accelerating targets without the need to manage cross-terms and without the computational overhead that the RAT, RWT and ICPF incur.

Detection performance of the proposed de-chirping method is compared to the integrated cubic phase function (ICPF) method for a single LFM signal. The same signal parameters as specified for Figure 7 of [9] are used to simulate the LFM signal, as follows.

$$x(n) = \exp\left\{j\left(0.1\pi + 0.2\pi n + \frac{0.1\pi}{N}n^2\right)\right\} + \nu(n), \quad n = \{0, 1, \ldots, N-1\}, \tag{10}$$

where the noise $\nu(n)$ is assumed to be complex white Gaussian noise with zero mean, $N = 64$ and the detection threshold was chosen to give a fixed probability of false alarm P_{fa} of 0.01.

The P_d plot of the Wang's report [9] is provided here as shown in Figure 10(a) and shows the probability of detection curves for the RWT, RAT and ICPF given the LFM signal described above.

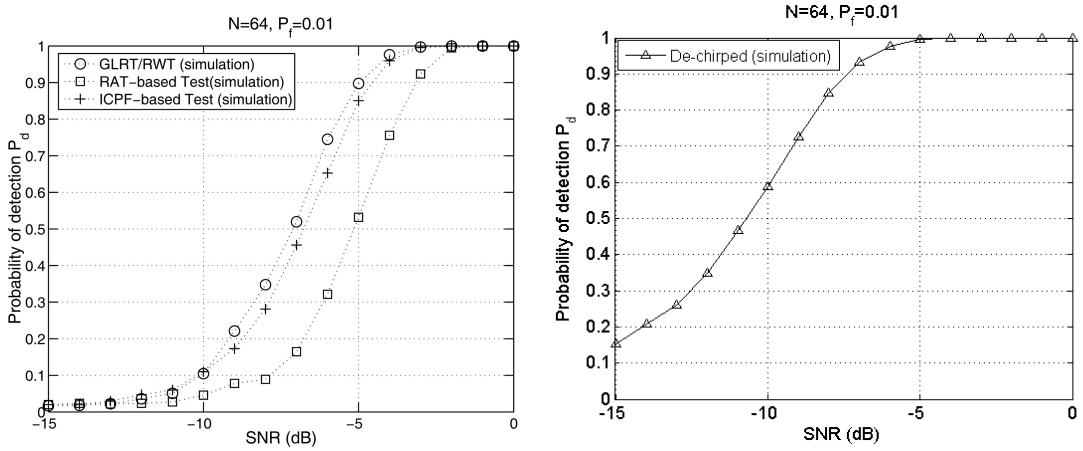

(a) RWT, RAT and ICPF techniques. Adapted from Wang *et al* [9]

(b) The de-chirping technique

Figure 10: *Comparison of detection performance of proposed de-chirping technique with known techniques.*

Figure 10(b) shows the probability of detection curve of our proposed dechirping technique, with the use of a standard CA-CFAR detector. As can be seen, at a typical $P_d = 0.5$, the dechirping technique provides an improvement of 5.6 dB compared with RAT processing, 3.8 dB compared to the ICPF technique, and 3.5 dB compared with the RWT. Alternatively, at a SNR of -10 dB, the detection performance of the dechirping technique over the RWT, RAT and ICPF are approximately 6, 12 and 5.5 times respectively. This

difference can be attributed to the added spurious false alarms and extra noise generated by significant cross-terms in the AF methods and ICPF at a fixed P_{fa} level. Cross terms arise between signals as well as between a signal and noise or between noise terms themselves. In the example used, although there is only one signal, cross terms between signal and noise, and between noise with noise itself has the effect of raising the noise floor.

As discussed in Section 3.1.2, the FrFT and dechirping technique produces an integration gain that is the same, and so we would expect the detection performance to be similar.

3.3.2 Computational Cost and Complexity

The performances of all processing techniques reviewed and described here are weighed up against their computational cost and algorithm complexity. Theoretically, the dechirping technique and FrFT calculations are $\mathcal{O}(N \log N)$ since they involve the multiplication of the signal with a chirp factor and a summation over time provided by the kernel function and FFT function respectively.

The AF and CPF calculations are also $\mathcal{O}(N \log N)$ [9] since they too involve a summation of the chirp factor multiplied with the time signal. However, both the AF and CPF techniques require further processing. The RWT and RAT techniques require the Radon transform to be applied, and with this additional processing the calculation is $\mathcal{O}(LN \log N)$ where L is the number of samples in the transformation. The ICPF involves an additional integration of the CPF over time, making the calculation $\mathcal{O}(MN \log N)$ where M is the number of time samples.

In terms of algorithm complexity, the dechirping technique, FrFT and ICPF detection processing all involve two 1D searches to determine the frequency and chirp-rate parameters where the estimate accuracy depends on the size of the frequency and chirp-rate grids used in the searches. For RWT and RAT processing, the radon transform calculation involves Cartesian-to-polar coordinate transformations and interpolations where the estimate accuracy depends, not only on the grid sizes, but also on how well the polar coordinates can be mapped to a rectangular grid in Cartesian space.

4 Results and Discussion

This section presents results for both simulated and real data for the detection problem *in clutter*. The simulated data results aim to show the compression effect and improvement in detectability of the target when the de-chirping technique is applied to an accelerating target when it is inside or outside a clutter region. The 'real' data results, due to limited availability, make use of two sets of data of mixed types: the first set consists of a simulated target in real sea clutter, and a second set contains a real target in simulated sea clutter. The aim of these datasets is to show, again, the spectral compression effect of the de-chirping technique and the defocussing effect of the de-chirping factor on real data, especially sea clutter.

4.1 Simulated Data Results

4.1.1 Single Target

We demonstrate the de-chirping technique using a simulated scenario involving a single target. A pulse Doppler radar operating at a frequency of 3 GHz with horizontal polarisation, with a pulse repetition frequency (PRF) of 40 kHz is mounted on a platform travelling at 100 m/s. The target is approaching the radar, nose aspect, at a constant acceleration of 30 m/s^2 and manoeuvres as depicted in Figure 11(a). The sea clutter characteristics are described as sea state 3[5]. The target at location A has maximum Doppler and falls well outside the clutter spectrum while at location B the targets instantaneous Doppler approaches zero and hence begins to fall into the clutter spectrum. These two extreme cases are further investigated.

Figure 11(b) and Figure 11(c) shows the spectra of the simulated target and clutter before and after the de-chirping technique has been applied respectively, for location A. For this location where the target is clearly outside the clutter, the target spread Doppler is easily seen and is 13 dB below the maximum clutter. After the de-chirping technique has been applied the resulting spectrum shows a well compressed spike for the target and a more broad spectrum for the clutter. The maximum clutter is now 15 dB below the target improving the detectability of the target.

Figure 11(d) and Figure 11(e) shows the spectra of the simulated target and clutter before and after the de-chirping technique has been applied respectively, for location B. For this location the target is inside the clutter. Similarly, the clutter dominates the target return in Figure 11(d) with the broad target spectrum overlapping the clutter return. After de-chirping has been applied, Figure 11(e), the target is compressed and the clutter is spread out. Again, detectability of the target has been improved with the target 16 dB above the maximum clutter.

Figure 12 is a performance comparison plot for a simulated target at location B with acceleration of 5g in simulated clutter. A target signal is generated such that the signal-to-clutter ratio (SCR) is set to 5 dB and the clutter-to-noise ratio (CNR) is set to 10 dB. The comparison is presented in terms of coherent integration gain as a function of CPI length. For 'bench marking' purposes, the FT of a non-accelerating target is also shown to show the maximum possible integration gain. For this case of relatively high SCR and SNR, the de-chirping technique gives results that are similar to the non-accelerating target case; i.e. gives maximum integration gain for a given CPI length.

Similarly, Figure 13 is a performance plot for a simulated target at location B with acceleration of 5g in simulated clutter, with a lower SCR set to 0 dB. The effects of clutter begin to dominate, with inaccurate estimates of the chirp-rate leading to only partial de-chirping of the signal and hence a degradation in the integration gain. However, the gain performance of the de-chirping technique is still significantly better than that of the traditional FT, especially at longer CPI lengths. Note that for this low value of SCR, the (random) gain component due to the incoherent integration of the clutter and noise in the total gain displayed in Figure 13 becomes more significant.

[5]Based on the Douglas Sea Scale

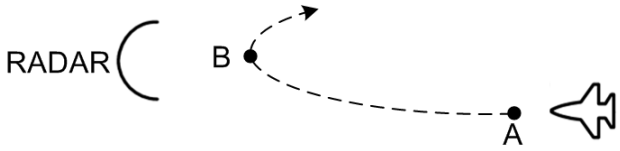

(a) Target trajectory in a test scenario. Target instantaneous velocities at locations A and B: 100 m/s and 0 m/s.

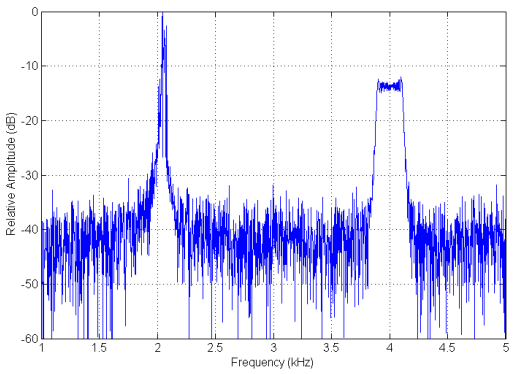

(b) Fourier spectrum of target and clutter when the target is at location A

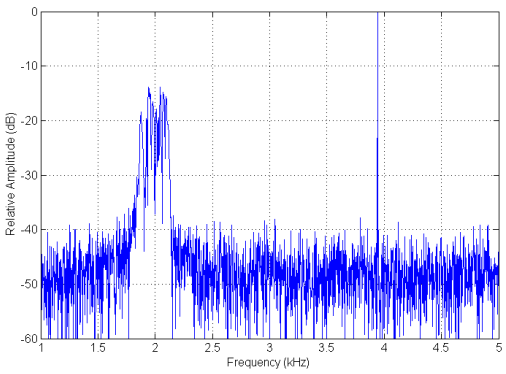

(c) De-chirped spectrum of target and clutter when the target is at location A and de-chirp rate matches the target acceleration

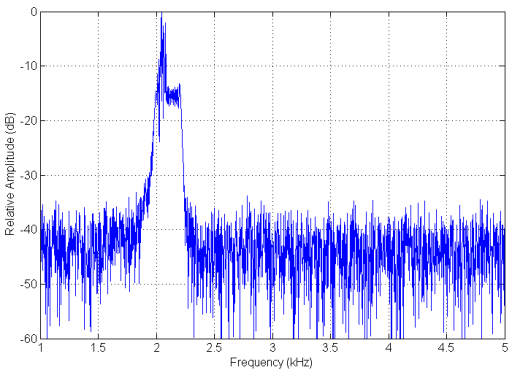

(d) Fourier spectrum of target and clutter when the target is at location B

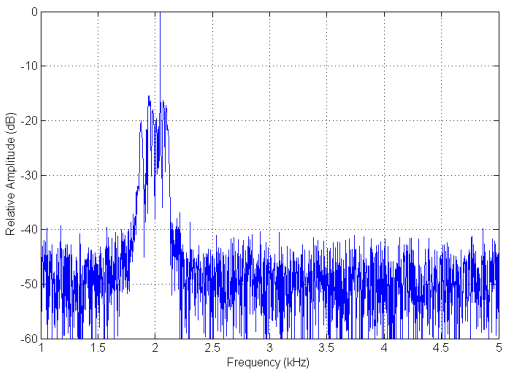

(e) De-chirped spectrum of target and clutter when the target is at location B and de-chirp rate matches the target acceleration

Figure 11: *Simulated target trajectory and Doppler spectra before and after application of the de-chirping technique.*

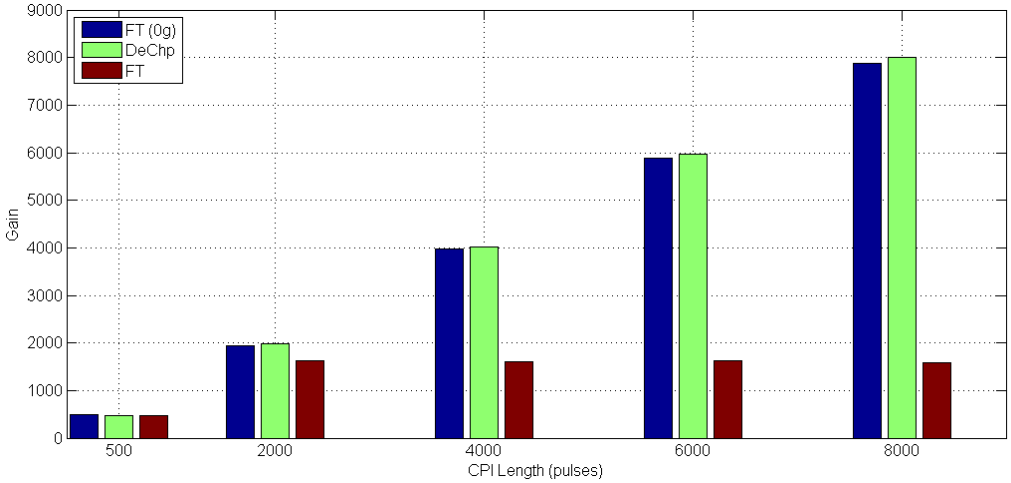

Figure 12: *Coherent integration gains of the FT and de-chirping techniques for a simulated target with acceleration of 5g, SCR = 5 dB.*

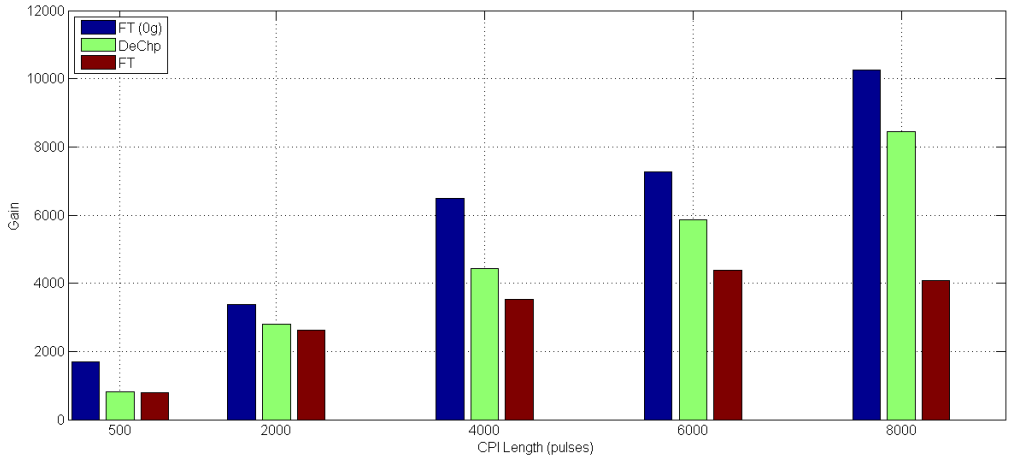

Figure 13: *Coherent integration gains of the FT and de-chirping techniques for a simulated target with acceleration of 5g, SCR = 0 dB.*

4.1.2 Multiple Targets

To demonstrate the detection algorithm for multiple targets, a similar simulated scenario is presented with three targets approaching the radar in the same range bin, in a certain CPI. However, their initial Doppler frequencies and accelerations are different, as follows:

- Target 1 has an initial velocity of 100 ms^{-1} (i.e. initial Doppler Frequency of 2 kHz), a constant acceleration of 5 ms^{-2} and relative signal-to-noise ratio of -4 dB,
- Target 2 has an initial velocity of 102 ms^{-1} (2.04 kHz), constant acceleration of 10 ms^{-2} and relative signal-to-noise ratio of -3 dB
- Target 3 has an initial velocity of 103 ms^{-1} (2.06 kHz), constant acceleration of 20 ms^{-2} and relative signal-to-noise ratio of -5 dB.

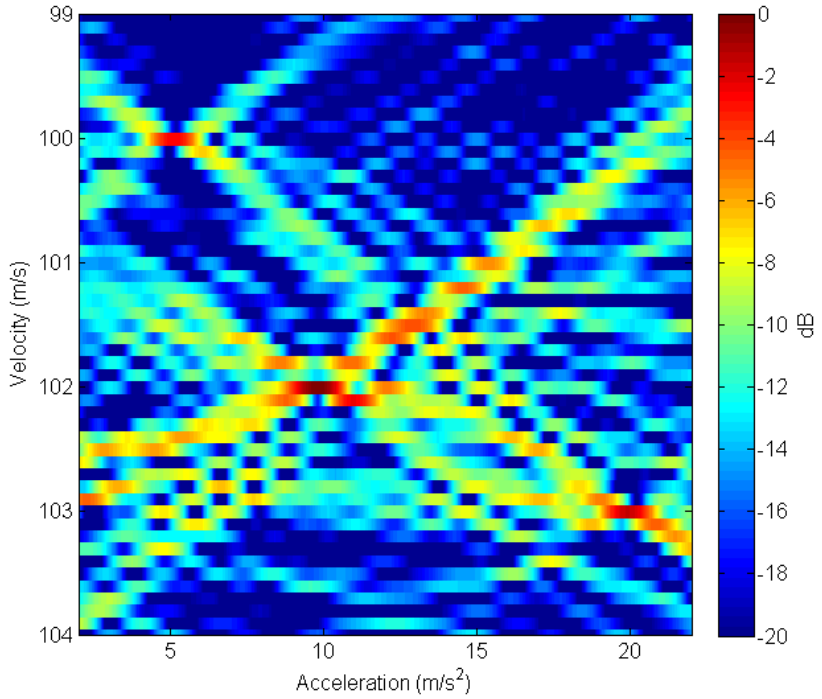

Figure 14: *A 2D velocity-acceleration plot of the signal after applying the de-chirping technique.*

To show an overview of the targets in the Doppler-acceleration space, the de-chirping technique is applied to the signal for a typical range of frequency and acceleration, resulting in a 2D plot as shown in Figure 14. For this plot we have labelled the x-axis and y-axis as acceleration and velocity respectively to better reflect the target parameters. The plot shows three major peaks corresponding to the signal strength and location of each target in this space. The other local maxima that appear in this 2D plot are caused from interference from all three targets. These maxima will generally be lower in magnitude than the compressed targets in low noise. However, in high noise conditions it is possible that constructive interference peaks can lead to false target detections. This problem highlights the need to use the CLEAN technique discussed in Section 3.2.2, in which the removal of a strong target after its detection would also remove possible interference with any other target in the signal.

By applying the de-chirping and CLEAN techniques, Figure 15 shows the successive spectra of the signal just before the detection of each target. Standard CFAR detection processing could be used for the individual detection step. Figure 15(a) shows the spectrum containing a frequency line optimally de-chirped, for the detection of the first (strongest) target, Target 2, which is approximately 10 dB above the clutter. The other two targets do not appear because they are defocussed at the de-chirp rate that is optimal for Target 2. Similarly, Figures 15(b) and 15(c) show the spectrum the next targets, Target 1 and Target 3. Note that the gains due to de-chirping, relative to standard processing, are roughly proportional to the true target accelerations. For Target 1 in this example, the

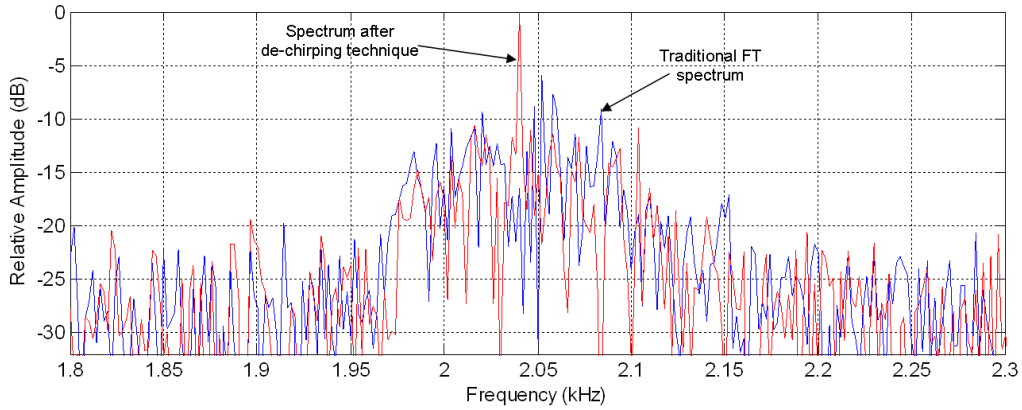

(a) The optimally de-chirped spectrum (red) to detect Target 2 (the strongest).

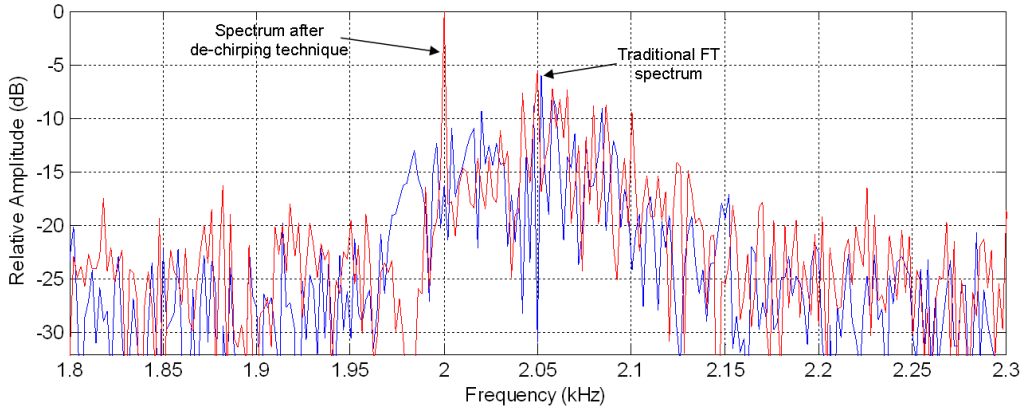

(b) The optimally de-chirped spectrum (red) to detect Target 1.

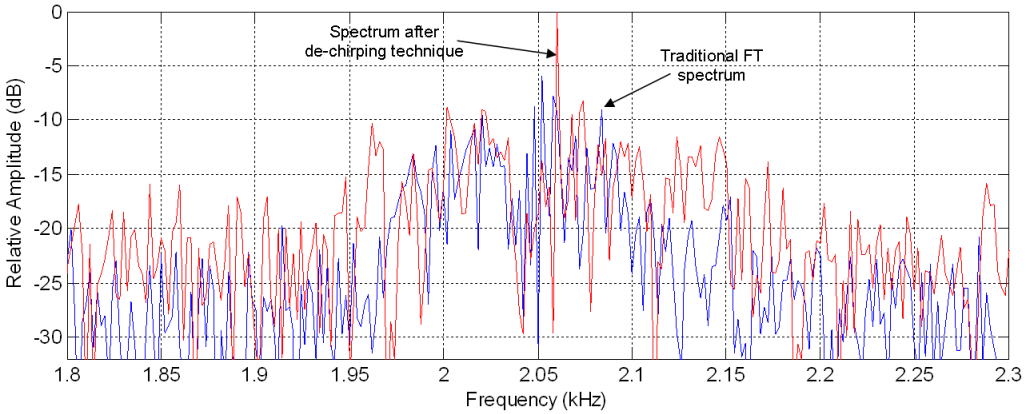

(c) The optimally de-chirped spectrum (red) to detect Target 3.

Figure 15: *Standard chirped (blue) and de-chirped spectra (red) to detect and extract each target, in the presence of clutter and noise.*

gain is approximately 8 dB above the clutter, while for Target 3, it is approximately 10 dB.

4.1.3 Computational Analysis

An analysis of the computational time for each function of the dechirping technique is presented to quantify the speed of the method. This was conducted using MATLAB R2013a on a PC running Windows 7 (64 bit) with a Intel Core i7 CPU operating at 3.4 GHz and equipped with 8 GB of RAM.

The processing time for each function from the single target and multiple target scenarios described in this section are measured and summarised in Table 2. The number of points for the chirp-rate and Doppler frequency grids are 800 and 10000 respectively giving accurate estimates for these parameters. However, a time saving can be achieved by reducing these grid sizes but this inevitably compromises estimate accuracy. Also, note that the CLEAN algorithm is only used in the multiple target processing and that the value presented in the table is the processing time per target.

Table 2: *Actual processing time for each function in the de-chirping technique.*

Function	**Processing Time (ms)**
Signal Dechirp	0.16
Chirp Rate Search	260
Doppler Freq. Search	250
CLEAN Algorithm per target	5.4

4.2 Real Sea Clutter Data

Here we present results of the de-chirping technique when applied to a simulated target in the presence of real sea clutter. The sea clutter data was collected during a trial in November 2006 on Kangaroo Island using an experimental van-mounted S-band radar developed by DSTO [26]. The low grazing angle measurement used a carrier frequency of 3.25 GHz with horizontal polarisation, PRF of 2.94 kHz and CPI of 0.34 s. The sea state was estimated to be between 3 to 4. The simulated target Doppler was placed inside the clutter spectrum with an acceleration of 20 m/s^2.

Figure 16 shows the spectra of a simulated target in real clutter before and after applying the de-chirping technique. As can be seen in the figure, the accelerating target remains below the clutter level in traditional FT processing. When the de-chirping technique is applied, coherent integration for the target signal is improved to an SCR of 9 dB approximately. Also, the clutter Doppler spread increases from 100 Hz to 200 Hz. The detectability of the accelerating target is indeed significantly improved with application of the de-chirping technique.

4.3 Real Target Data

Here we present results of the de-chirping technique when applied to a real target (a Bell 206 helicopter with a small acceleration) in the presence of simulated clutter. The

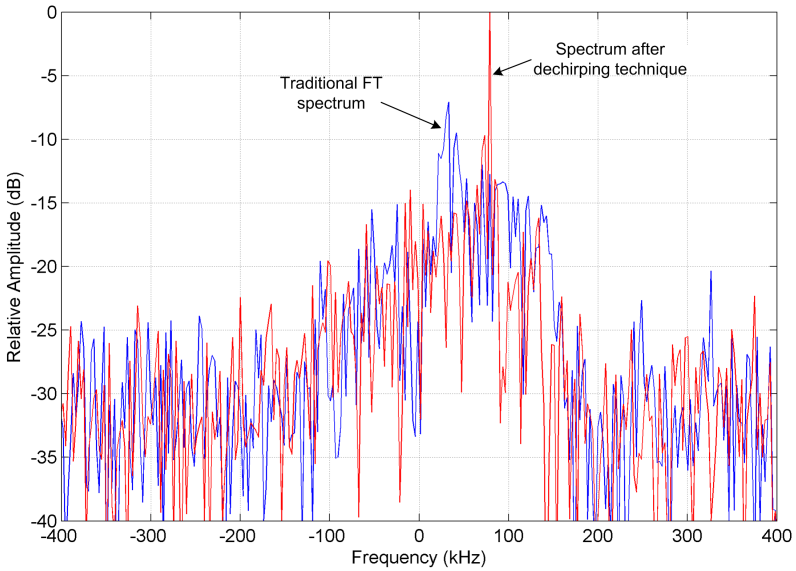

Figure 16: *Spectra of a simulated target in real clutter with traditional FT processing and with the de-chirping technique.*

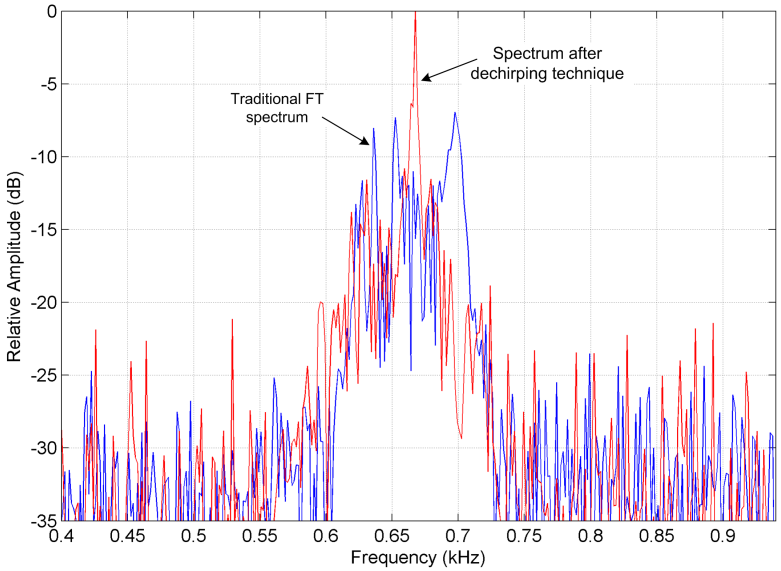

Figure 17: *Spectra of a real target in simulated clutter with traditional FT processing, and with the de-chirping technique.*

helicopter target data was collected during a trial in May 2011 using a van-mounted experimental X-band radar operating at a carrier frequency of 9.5 GHz, horizontal polarisation, and with a PRF of 33.3 kHz. To ensure the target acceleration remained approximately constant during coherent integration, a maximum CPI length of 0.64 s was chosen.

Figure 17 shows the spectra of a real target in simulated clutter before (i.e. with FT processing only) and with the de-chirping technique applied. The clutter is simulated sea clutter of sea state 5, with an SCR of 3 dB. A couple of features of interest can be noted here. Firstly, the target is compressed to approximately 12 dB above clutter, while with standard FT processing, the target is buried in clutter. Secondly, with a target acceleration of only 2.2 $\mathrm{m/s^2}$ as estimated by the de-chirping process for this particular example, the defocussing of clutter under the action of the de-chirping factor is not pronounced, and hence does not significantly contribute to the SCR enhancement. For many real manoeuvring targets with high acceleration and a modest CPI, a significant processing gain can be achieved through target focusing and clutter defocussing.

5 Conclusion

We have shown that the simple de-chirping technique is a fast and effective tool for detecting accelerating targets in clutter, where the traditional Fourier transform may fail. Its performance is essentially the same as the more novel FrFT technique; they both can achieve the maximum coherent integration gain as in the case for the traditional Fourier transform on pure tone signals, as well as in defocussing the clutter component. In terms of computational cost, the de-chirping technique is faster than the FrFT, although both techniques are $\mathcal{O}(N \log N)$. These results have been confirmed with real data.

The proposed linear technique also performs favorably compared to bilinear techniques reported earlier in the literature, because no cross-terms are involved in the processing and thus no added spurious false targets are generated in the processed signal. A comparison is made for a single component LFM signal, and further analysis with real data is recommended to compare the proposed technique with existing bilinear techniques.

For multiple accelerating targets present in the same range bin, we have illustrated an efficient algorithm for their detection, based on the de-chirping technique and the CLEAN algorithm. Comparison of detection performance with the integrated cubic phase function method in the case of multiple LFM targets is beyond the scope of the current study and will be revisited in a future investigation. Nevertheless, the proposed technique, with its linear nature, is most likely a promising detector. Future work will also investigate the range-walk problem, where a target may extend across multiple range-bins during a CPI.

Acknowledgements

We sincerely thank Prof. Doug Gray of the University of Adelaide for a stimulating discussion, Mr. Gavin Currie for his great help in generating the simulated clutter data, Dr. Giuseppe Fabrizio for critically reviewing this work and providing helpful comments,

and Dr. Andrew Shaw (Research Leader, Surveillance and Reconnaissance Branch, DSTO Edinburgh) for his review, leadership and support.

References

1. Abatzoglou, T.J., *"Fast Maximum Likelihood Joint Estimation of Frequency and Frequency Rate"*, IEEE Transactions on Aerospace and Electronic Systems 22, 708-715, 1986.

2. Peleg, S. and Porat, B., *"Linear FM signal parameter estimation from discrete-time observations"*, IEEE Transactions on Aerospace and Electronic Systems 27(4), 607-616, 1991.

3. Wood, J.C. and Barry, D.T., *"Radon transformation of time-frequency distributions for analysis of multicomponent signals."*, IEEE Transactions on Signal Processing, 42(11), 31663177, 1994.

4. Barbarossa, S., *"Analysis of multicomponent LFM signals by a combined Wigner-Hough transform."*, IEEE Transactions on Signal Processing, 43(6), 15111515, 1995.

5. Wang, M., Chan, A.K., and Chui, C. K., *"Linear frequency-modulated signal detection using radon-ambiguity transform."*, IEEE Transactions on Signal Processing, 46(3), 571586, 1998.

6. Wang, P. and Yang, J., *"Multicomponent chirp signals analysis using product cubic phase function."*, Digital Signal Processing, 16(6), 654669, 2006.

7. OShea, P., *"A fast algorithm for estimating the parameters of a quadratic FM signal."*, IEEE Transactions on Signal Processing, 52(2), 385393, 2004.

8. Wang, P., Djurovic, I., and Yang, J., *"Generalized high-order phase function for parameter estimation of polynomial phase signal."*, IEEE Transactions on Signal Processing, 56(7), 30233028, 2008.

9. Wang, P., Li, H., Djurovic, I., Himed, B., *"Integrated Cubic Phase Function for Linear FM Signal Analysis"*, IEEE Transactions on Aerospace and Electronic Systems, 46(3), 2010.

10. Melino R. and Tran H.T., *"Application of the Fractional Fourier Transform in the Detection of Accelerating Targets in Clutter"*, DSTO Research Reports, DSTO-RR-0365, April 2011.

11. Capus, C., *"Short-time fractional Fourier methods for the time-frequency representation of chirp signals"*, Journal of Acoustical Society of America, Vol. 113, No. 6, June 2003.

12. Chen, X. and Guan, J., *"A fast FRFT based detection algorithm of multiple moving targets in sea clutter"*, 2010 IEEE Radar Conference, 2010, pp.402-6.

13. Swerling, P., *"Probability of detection for fluctuating targets"*, The RAND Corporation, Research Memorandum RM-1217, March 17, 1954.

14. Yasotharan A., and Thayaparan T., *"Strengths and limitations of the Fourier method for detecting accelerating targets by pulse Doppler radar"*, IEE Proceedings - Radar Sonar Navigation, Vol 149, No.2, April 2002, pp. 83-88.

15. Defence Evaluation and Research Agency UK, *"Naval Environmental Clutter, Attenuation and Propagation Specification - NECAPS 3"*, DERA/SS/CS/WP000023/1.0.

16. Lohmann, A.W. and Soffer, B. H., *"Relationships between the Radon-Wigner and fractional Fourier transforms"*, Journal of Optical Society of America, Vol. 11, No. 6, June 1994.

17. Namias, V., *"The fractional Fourier transform and its application to quantum mechanics"*, J. Inst. Math. Appl., Vol.25, pp.241-65, 1980.

18. Tran H.T., and Melino R., *"Application of the fractional Fourier transform and S-method in Doppler radar tomography"*, DSTO Research Report, DSTO-RR-0357, August 2010.

19. Akay, O. and Erozden, *"Emplying fractional autocorrelation for fast detection and sweep rate estimation of pulse compression radar waveforms"*, Signal Processing 89, 2479-2489, 2009.

20. Clarkson, V. L., *"Tone and chirp detection using sums of conjugate products"*, in Australasian Workshop on Signal Processing Applications, pp. 189-192, 1997.

21. Amblard, P. O., Brossier, J.-M. *"Adaptive estimation of the fourth-order cumulant of a white stochastic process"*, Signal Processing, Vol.42, pp.37-43, 1995.

22. Qin, Y., Wenyao, L., Shouli, Z., Hairon, H., *"Detection of Chirp Signal by Combination of Kurtosis Detection and Filtering in Fractional Fourier Domain"*, 2nd International Congress on Image and Signal Processing, pp.1-6, 2009.

23. Mallat, S. and Zhang, Z., *"Matching pursuit with time-frequency dictionaries"*, IEEE Transactions on Signal Processing 41(12), 3397-3415, 1993.

24. Qian, S. and Chen, D., *"Signal representation using adaptive normalized Gaussian functions"*, Signal Processing 36, 1-11, 1994.

25. Gribonval, R., *"Fast matching pursuit with a multiscale dictionary of Gaussian chirps"*, IEEE Transactions on Signal Processing 49(5), 994-1001, 2001.

26. Dong, Y. and Merrett, D., *"Statistical measures of S-band sea clutter and targets"*, 2008 International Conference on Radar, pp. 575-580, October 2008.

THIS PAGE IS INTENTIONALLY BLANK

DEFENCE SCIENCE AND TECHNOLOGY ORGANISATION DOCUMENT CONTROL DATA	1. CAVEAT/PRIVACY MARKING

2. TITLE	3. SECURITY CLASSIFICATION
Detection of Accelerating Targets in Clutter Using a De-Chirping Technique	Document (U) Title (U) Abstract (U)
4. AUTHORS	5. CORPORATE AUTHOR
H.T. Tran, R. Melino, and S. Kodituwakku	Defence Science and Technology Organisation PO Box 1500 Edinburgh, South Australia 5111, Australia

6a. DSTO NUMBER	6b. AR NUMBER	6c. TYPE OF REPORT	7. DOCUMENT DATE
DSTO–RR–0399	AR-015-961	Research Report	June, 2014

8. FILE NUMBER	9. TASK NUMBER	10. TASK SPONSOR	11. No. OF PAGES	12. No. OF REFS
2013/1118140/1	07-044	HASD	27	26

13. URL OF ELECTRONIC VERSION	14. RELEASE AUTHORITY
`http://www.dsto.defence.gov.au/publications/scientific.php`	Chief, National Security and Intelligence, Surveillance and Reconnaissance Division

15. SECONDARY RELEASE STATEMENT OF THIS DOCUMENT

Approved for Public Release

OVERSEAS ENQUIRIES OUTSIDE STATED LIMITATIONS SHOULD BE REFERRED THROUGH DOCUMENT EXCHANGE, PO BOX 1500, EDINBURGH, SOUTH AUSTRALIA 5111

16. DELIBERATE ANNOUNCEMENT

No Limitations

17. CITATION IN OTHER DOCUMENTS

No Limitations

18. DSTO RESEARCH LIBRARY THESAURUS

De-chirping technique, Linear chirp detection, Accelerating target, Pulsed Doppler radar

19. ABSTRACT

Accelerating targets induce chirped signals in the radar backscatter signal which cannot be efficiently detected by the direct application of the traditional Fourier transform. In this report, we propose a method based on a de-chirping factor and the Fourier transform for detecting accelerating targets in land or sea clutter environments. The method is found to be simple, yet highly effective. The results are demonstrated with both simulated and real data.